DOI: 10.13009/EUCASS2019-671

Elastic waves simulation and damping characterization on composite structures for structural health monitoring applications.

Fernando Sánchez Iglesias⋆†, *Pablo Broncano García*⋆, *Rubén Tejerina Hernanz*⋆,
Antonio Fernández López⋆⋆ and Manuel Iglesias Vallejo⋆
⋆ *Airbus Defence and Space*
P. John Lennon, S/N, 28906, Getafe (Madrid), Spain
⋆⋆ *Technical University of Madrid*
Plaza Cardenal Cisneros, 328040, Madrid, Spain
fernando.i.sanchez@airbus.com · pablo.broncano-garcia@airbus.com
† Corresponding author

Abstract

A study based on the numerical simulations of the propagation of elastic waves on composite panels has been performed in order to support the development of a Structural Health Monitoring system.
The simulations are correlated with a number of active interrogation tests, which have been performed in both a simplified composite plate and a representative aircraft structure. Additionally passive tests of very low energy impacts have also been used to estimate a damping coefficient to use in the simulations. The results and validation of the simulations are discussed in this paper.

1. Introduction

The use of composite materials in the aerospace industry is becoming more prevalent in current aircraft developments due to their potential advantages in weight specific strength, stiffness and good fatigue and corrosion resistance and are replacing the classical metallic material structures in many areas.[2,5] However, these materials may require some special attention as they present a very poor impact resistance and a much wider range of failure modes, most of them not easy to be detected by visual inspection.[9,15,20,21] For this reason, new and affordable inspection systems must be developed to be able to study the performance of these structures in service.

The work presented in this paper is part of the roadmap of simulation activities for SHM systems development for Airbus Defence and Space, previously presented in[10] . Airbus Defence and Space in collaboration with UPM is researching topics that might be applied into a future structural health monitoring systems covering also composite structures; the extraction of damage-sensitive features from the measurements of a sensor array appropriately installed on the structure, and the analysis of these features can be used to determine the current state of the structure health. The information can be used for other purposes within the system functionalities being prescribed such as real time events detection. These structural health monitoring systems could present many cost advantages when compared with the traditional inspection methods, and could also be used to improve the life prediction of the structure based on its usage.

This paper focuses on the usage of piezoelectric sensors to study the response of the structure elastic waves as a possible inspection method that could be used on a structural health monitoring system. In order to set up this system, a huge effort is required to address all the possible events and damage scenarios, ideally via physical testing although virtual testing, after test correlation, is also valid. The results of a set of numerical simulations based on an explicit finite element analysis code are presented in this paper; these simulations can provide an accurate prediction of the behavior of the structure under a wide range of different scenarios, which is necessary for developing a robust structural health monitoring system.

DOI: 10.13009/EUCASS2019-671

The simulations are based on both a simple plane composite plate and a representative section of the Green Regional Aircraft (GRA) demonstrator cockpit developed within Clean Sky's Airbus Defence and Space collaboration boundaries, in which the system has also been installed and in both cases focuses on the active emission of the piezoelectric sensors. The results of the simulations at the location of the piezoelectric sensors are compared with a complex battery of physical tests that has been performed on both the GRA cockpit and the flat composite plate. These tests, which are also presented in the paper, are used to gain a better understanding of the problem and validate the simulation. The match between the tests and the simulation has been acceptable in most of the cases studied.

Additionally, the piezoelectric sensor array may also perform, in a passive way in order to detect elastic waves in the structure that could be produced by different sources. Impact as one of these sources, is being investigated in combination with other structural characteristics (i.e damping) to adjust the elastic waves signals content in the simulations to better match the tests. In order to characterize its energy and estimate the possibility of damage using this piezoelectric sensor array, different impact energy tests have been performed on the structural component.

1.1 Guided Lamb waves

In general, elastic waves in solid materials are guided by the boundaries of the media in which they propagate. Waves in metallic plates were among the first guided waves to be analyzed in 1917 by Horace Lamb;[14] the characteristic equations were established for waves propagating in an infinite plate and describe two modes of propagation: symmetric (S0) and antisymmetric (A0):

$$\text{Symmetric mode}: \frac{\tan qh}{\tan ph} = -\frac{4k^2qp}{(k^2-q^2)^2}$$

$$\text{Antisymmetric mode}: \frac{\tan qh}{\tan ph} = -\frac{\left(k^2-q^2\right)^2}{4k^2qp}$$

$$p^2 = -\frac{\omega^2}{c_L^2} - k^2,\ q^2 = -\frac{\omega^2}{c_T^2} - k^2,\ \text{and}\ k = \frac{\omega}{c_p}$$

where h, k, c_L, c_T, c_P and ω are the plate thickness, wavenumber, velocities of longitudinal and transverse modes, phase velocity and wave circular frequency, respectively. This equation implies that Lamb waves, regardless of mode, are dispersive.

These propagation modes are shown in Figure 1.

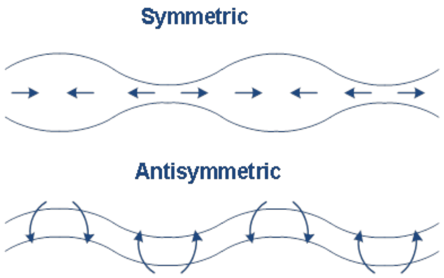

Figure 1: Lamb wave propagation modes

Lamb waves differ from the standing waves as the particle motion at an arbitrary point in space is not periodic, they are then a particular case of traveling waves. By definition, Lamb waves have no particle motion in the transversal direction. This motion is found in the so-called shear wave modes (Sh), which have no motion in the longitudinal or vertical directions, and are thus complementary to the Lamb wave modes.

Lamb waves traveling in composite thin plates are very sensitive to defects or damages.[17] This opens a wide field of applications for structural health monitoring, especially for composite structures, as they are prone to damages such as delaminations, not easily detected by visual inspection techniques; or structures for space applications that cannot be inspected during their service life ([11,16]).

DOI: 10.13009/EUCASS2019-671

1.2 Damping in composite materials

Damping mechanisms in composite materials are different, more complex and usually more severe than those from conventional metals. This is due to the multiple energy dissipation sources that can be present in a composite structure and are not present in metals, such as:

- The viscoelastic nature of the matrix. Usually, the major contributor to the damping of the laminate,[3] although the damping of the fibers may also be significant in some cases.
- Intephase damping. The interphase between the fiber and the matrix presents some unique characteristics and in some cases a significant thickness that may influence the damping of the composite.[7]
- Damping due to damages or imperfections. Composite materials are usually more prone to damages than traditional metallic strucutres; even when these damages may be small and negligible form a structural point of view, they can still dissipate energy and present some special mechanisms unique to composites.
- High vibrations. Viscoelastic damping is another unique characteristic of composite materials.[12]
- Temperature changes that may produce thermo-elastic damping.[4,12]

In the case of impact detection, the damping characteristics of a structure become crucial in the response measured in the piezo-electric sensors. Attempts to characterize damping parameters on composite materials to be used in a numerical simulation have been done previously as in,[8] however in this case, a different approach is taken studing the passive response of the sensors under the impact excitation.

2. Methodology

2.1 Experimental set-up

To validate the simulations and gain a better understaing of the propagation of elastic waves on aeronautic structures, the testing campaign, performed by the Technical University of Madrid, has been designed for two different representative structures, namely:

- A simplified structure, consisting on a square composite panel, instrumented with 8 piezoelectric sensors.
- A section of the GRA demonstrator cockpit, consisting on the skin and an omega stiffener, instrumented with 10 piezoelectric sensors.

DOI: 10.13009/EUCASS2019-671

2.1.1 Flat panel

Both active pitch/catch interrogation and passive impact tests have been performed on a square composite plate, shown in Figure 2a. The position of the piezoelectric sensors is shown in Figure 2b.

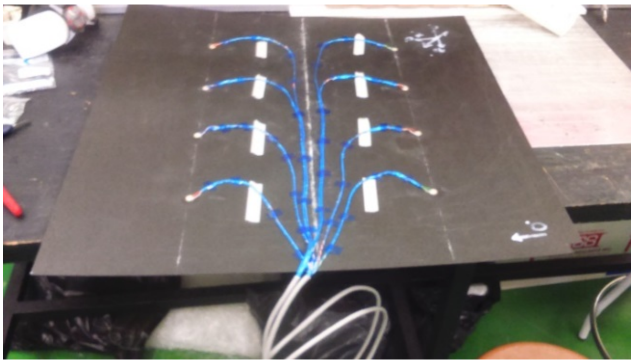

(a) Flat panel composite specimen tested.

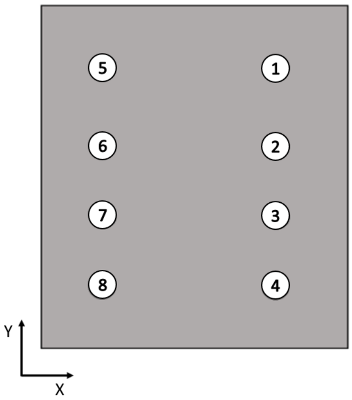

(b) Position and numbering of the piezoelectric sensors on the flat panel composite specimen.

Figure 2: Flat panel experimental test set-up

For the active interrogation tests the data is recorded using and ACELLENT SCANGENIE data acquisition card on a frequency range between 50 kHz and 500 kHz with a 50 kHz step, combining all possible emitting and receiving paths, this generates a total of 560 signals. Although, for the validation with the simulation only the tests at 200kHz are used.

The passive impact tests are done on the non-stiffened plate using a Brüel and Kjær instrumented hammer model 8206-003 and the piezoelectric signals and hammer load cell are recorded with a National Instruments data acquisition card model NI-USB-6366, as shown in Figure 3. The hammer has both an aluminium tip and a rubber tip.

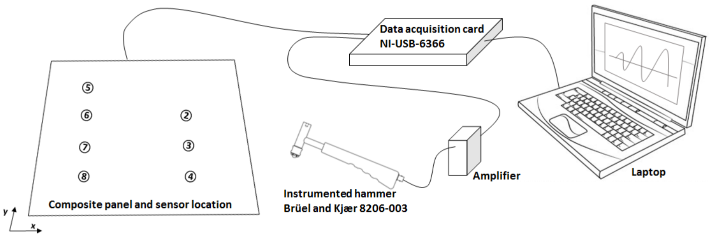

Figure 3: Hammer impact tests definition.

DOI: 10.13009/EUCASS2019-671

2.1.2 GRA cockpit tests

In the framework of the European Research Program Clean Sky - Green Regional Aircraft (GRA) integrated technology development, Airbus DS is commited to the development of technologies aimed for weight average reduction of 8% of aeronautic structures to contribute to meet the "green" requirements of future regional aircraft. In this framework, Airbus DS integrated these technologies in the GRA cockpit shown in Figure 4.

Figure 4: Green regional aircraft demonstrator cockpit

The cockpit is instrumented in many areas that may be prone to impacts with piezo-electric sensors as shown in Figure 5, and similar active interrogation tests are also perfomed on it.

Figure 5: GRA instrumented skin section.

DOI: 10.13009/EUCASS2019-671

The simulated area is instrumented with 10 piezoelectric sensors as shown in Figure 6. A composite omega stiffener is located between the two rows of sensors.

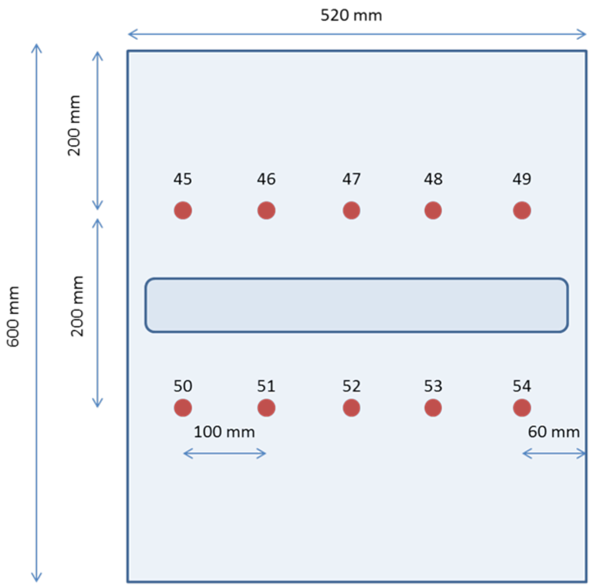

Figure 6: Simulated GRA panel and stiffener

2.2 Rayleigh damping model

While damping may not be significant for the active test, it is critical to understand the evolution of the signal for the passive detection system.

The Rayleigh or proportional damping model ([19])) defines the damping matrix $[C]$ as a factor α times the mass matrix, $[M]$, plus a factor β times the stiffnes matrix $[K]$; this model has been applied in[8, 18] for lamb wave simulations as it is very computationally efficient. On a one degree of freedom system gives the critical damping ratio ζ as:

$$[C] = \alpha\,[M] + \beta\,[K] \implies \zeta = \frac{1}{2}\left(\frac{\alpha}{\omega_n} + \beta\omega_n\right) \tag{1}$$

where ω_n is the natural frequency and α and β are two parameters of the damping model.

Assuming that the structure will behave as an under-damped system, as it is the case in most aeronautic applications, the response $V(t)$ measured at a sensor could be described with the following equation:

$$V(t) = \mathrm{e}^{-\omega_n \zeta t}\left(V_0 \cos\omega_D t + \frac{\dot{u}_0 + \zeta\omega_n u_0}{\omega_D}\sin\omega_D t\right) \tag{2}$$

where ω_D is the damped natural frequency, such as: $\omega_D = \omega_n\left(1-\zeta^2\right)^{1/2}$

The absolute area of the previous equation results in:

$$A = -A_0\mathrm{e}^{-\omega_n\zeta t} + C = -A_0\exp\left(-\omega_n t\left(\frac{\alpha}{2\omega_n} + \frac{\beta\omega_n}{2}\right)\right) + C \tag{3}$$

where A_0 is defined as a funtion of the average absolute voltage, V_0, as $A_0 = -V_0/\left(\omega_n\zeta\right)$, and C is a constant.

The parameter β mostly affects the oscillations at high frequency, therefore taking $\beta = 0$ the previous equation can be written as:

$$A = A_0\mathrm{e}^{-\alpha t} + C \tag{4}$$

From which the α parameter can be easily extracted by fitting the equation to the measured response from the tests.

DOI: 10.13009/EUCASS2019-671

2.3 Finite element model description

The Finite Element Method (FEM) analysis is done with Abaqus/Explicit version 2017 following the same methodology described in.[10] The composite solid panel is represented with continuum shell elements (SC8R) and conventional 2D shell elements (S4R) are used for the piezoelectric sensors/actuators. As the simulation must be able to represent the elastic wave behavior as it progresses through the panel an average element length of 1 mm is used in the model; this ensures that an antisymmetric wave up to a frequency of 200 kHz can be captured by the model using at least 10 elements per wavelength.[13,22]

The size limitation to model the elastic wave results in a very large mesh, of around 600 000 elements and 1 500 000 nodes. The mesh has been generated approximately uniform for most of the panel, however, because of the rounded shape of the piezoelectric sensor, it is distorted at those points as shown in Figure 7.

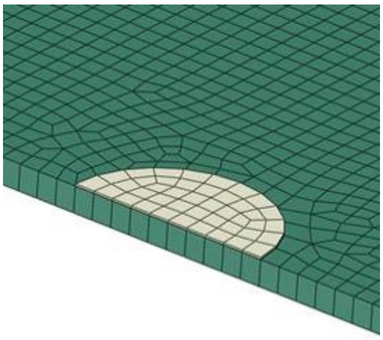

Figure 7: PZT sensor FEM model mesh detail.

In order to obtain the signal in the piezoelectric sensors, the stress measured in the finite element model elements must be converted to voltage. The following relationship can be applied to obtain the electric voltage contribution that could be generated by each element i, assuming that the sensor is working on its linear range[1,6] :

$$V_i = \frac{d_{31}(T_1 + T_2)}{\epsilon_0} \cdot h \tag{5}$$

were T_1 and T_2 are the element stresses in directions 1 and 2, h is the piezoelectric sensor thickness, ϵ_0 is the electric constant and d_{31} is the piezo-electric constant, taken from previous validated experimental data.

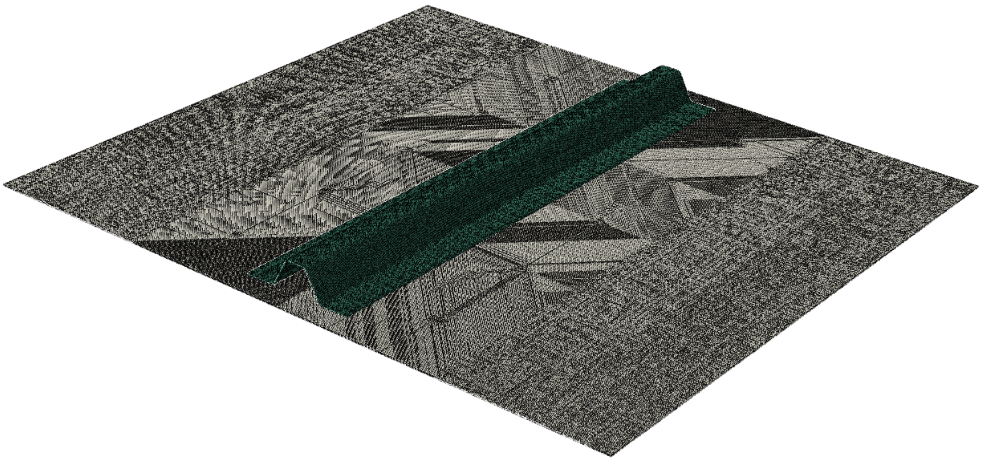

Figure 8: GRA panel FEM model.

DOI: 10.13009/EUCASS2019-671

3. Results and discussion

3.1 Damping model adjustment

An example of the fitting of A_0, ζ' and C is shown in Figure 9a. The time for the fitting is limited to 0.3 s sufficient to developt the majority of the impact energy in every case. Taking its derivative the curve can be plotted alongside the time history of the impact as shown in Figure 9b.

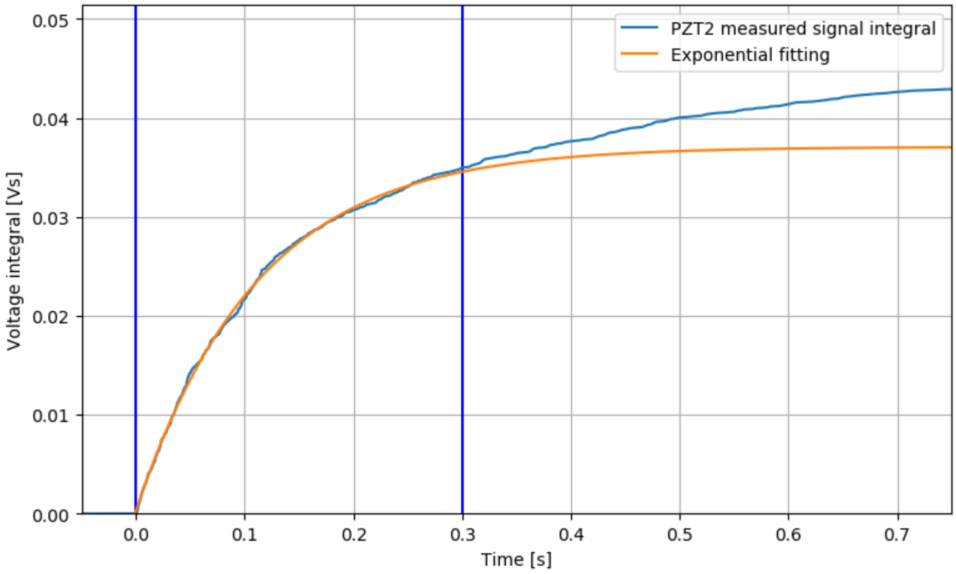

(a) Integral of the signal

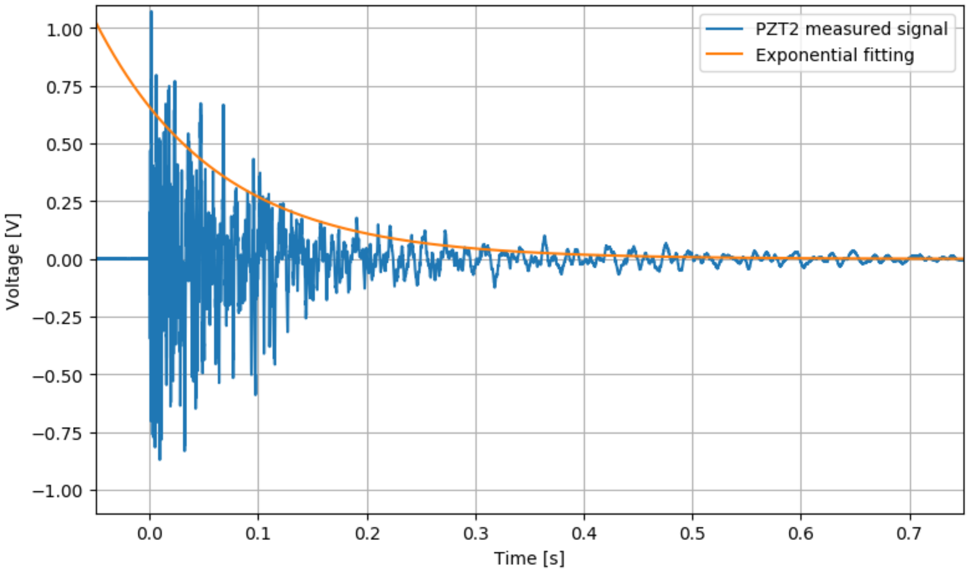

(b) Sensor signal

Figure 9: Exponential fitting adjustment of the piezoelectric sensor signals

The results from applying the fitting to all the cases studied are shown in Table 1.

Table 1: Damping parameter results for each impactor tested

	N. of cases	α	std (α)
Aluminium tip	98	8.783 Hz	9.142
Rubber tip	42	4.962 Hz	2.551

Therefore it proposed to use the following Rayleigh damping parameters for the FEM simulation: $\alpha = 7.63$ Hz and $\beta = 0.0$ s.

3.2 Active interrogation results

The vertical displacement results of the flat panel simulation at $t = 0.068$ ms while emitting a 200 kHz BURST-3 signal from PZT2 is shown in Figure 10. The different propagation modes are identified in the figure.

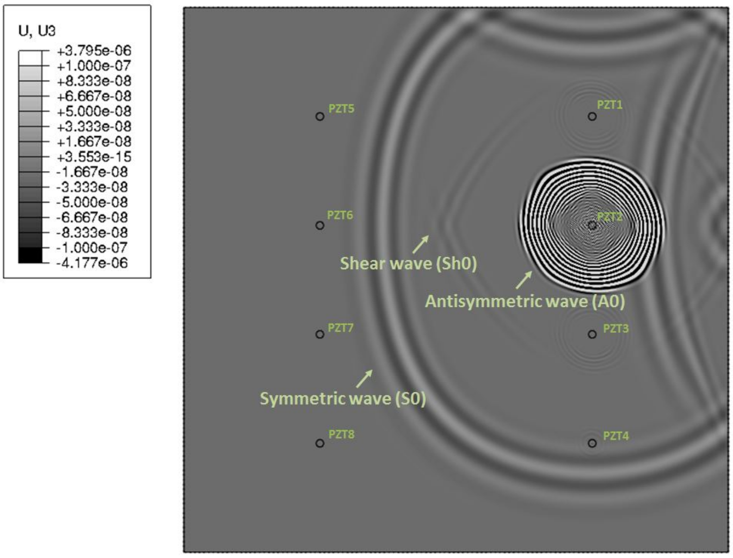

Figure 10: Active interrogation results for the flat composite panel - Actuator PZT2.

DOI: 10.13009/EUCASS2019-671

The comparison of the active interrogation signals for the flat panel is presented in Figures 11 and 12 duplicated or redundant paths are not shown. Paths between consecutive sensors/actuators are also not shown, as the crosstalk overlaps the symmetric wave on the experimental results.

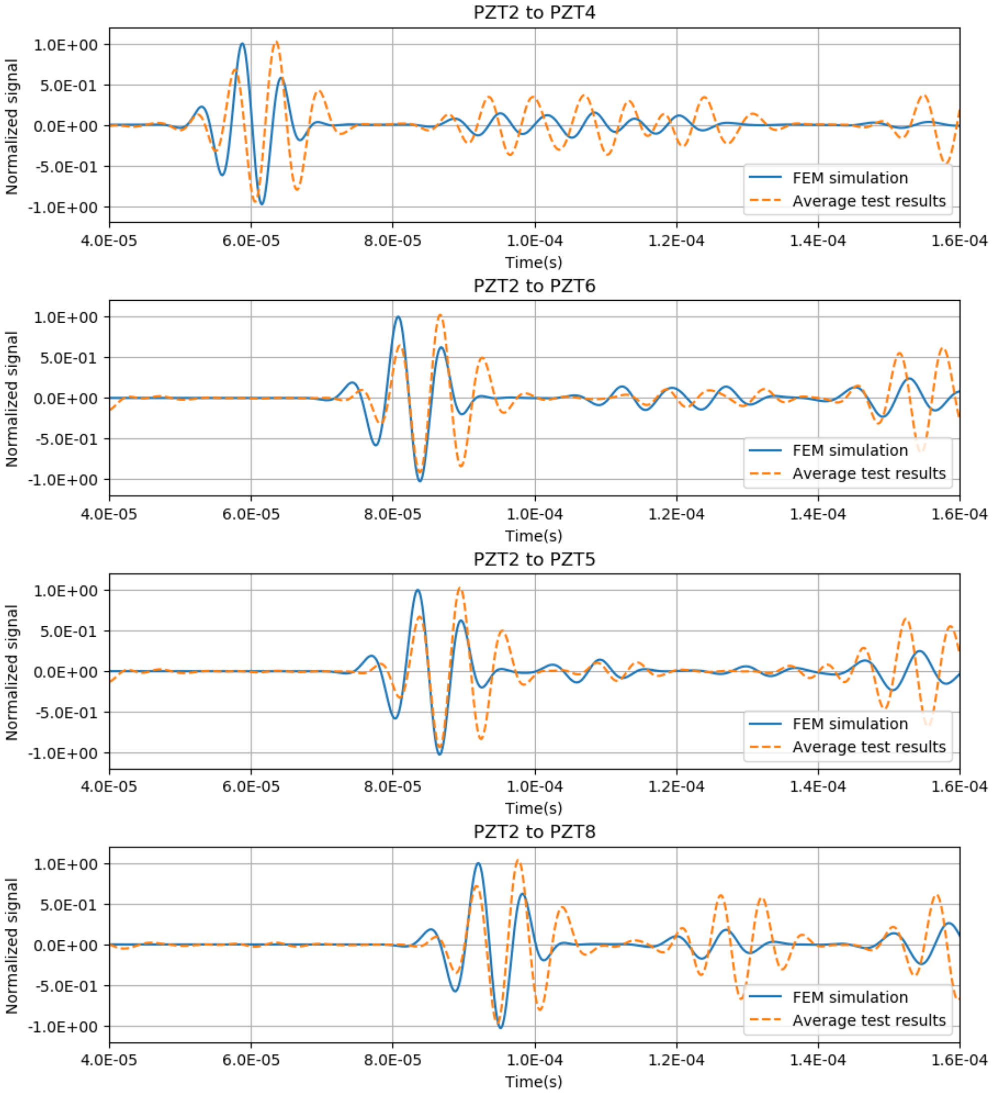

Figure 11: Active interrogation results for the flat composite panel - Actuator PZT2.

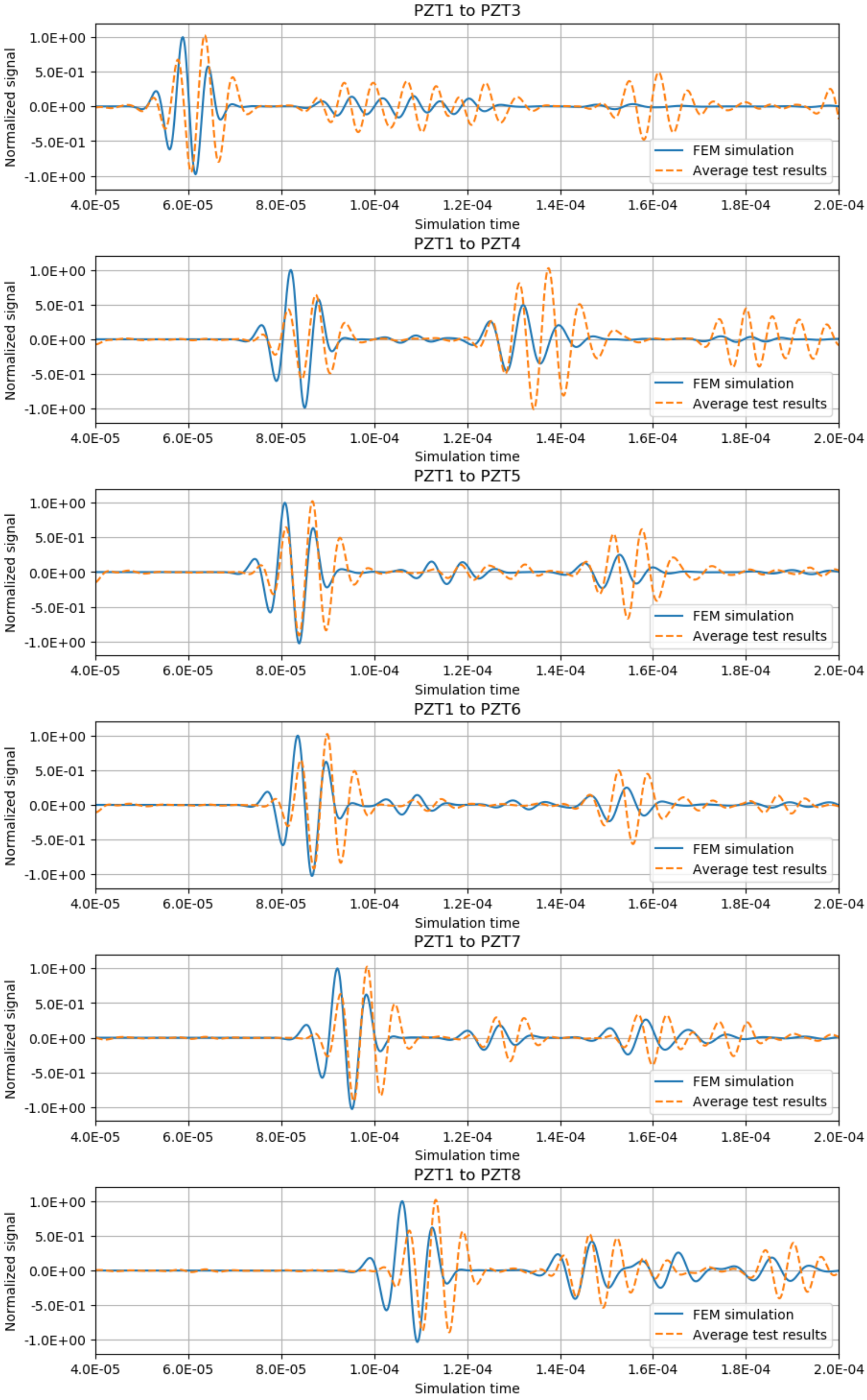

Figure 12: Active interrogation results for the flat composite panel - Actuator PZT1.

The vertical displacement results of the GRA panel simulation at $t = 0.05$ ms while emitting a 200 kHz BURST-5 signal from PZT47 is shown in Figure 13; as with the flat panel, the different propagation modes are identified in the figure. The results for a number of relevant paths are shown in Figures 14, 15 and 16.

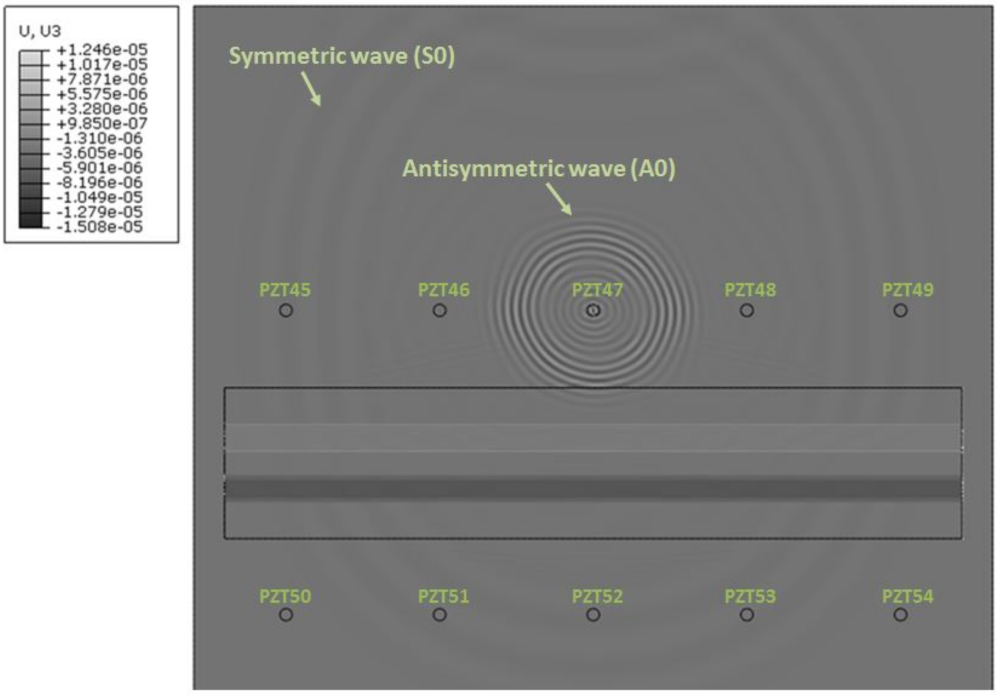

Figure 13: Active interrogation results for the GRA panel - Actuator PZT47.

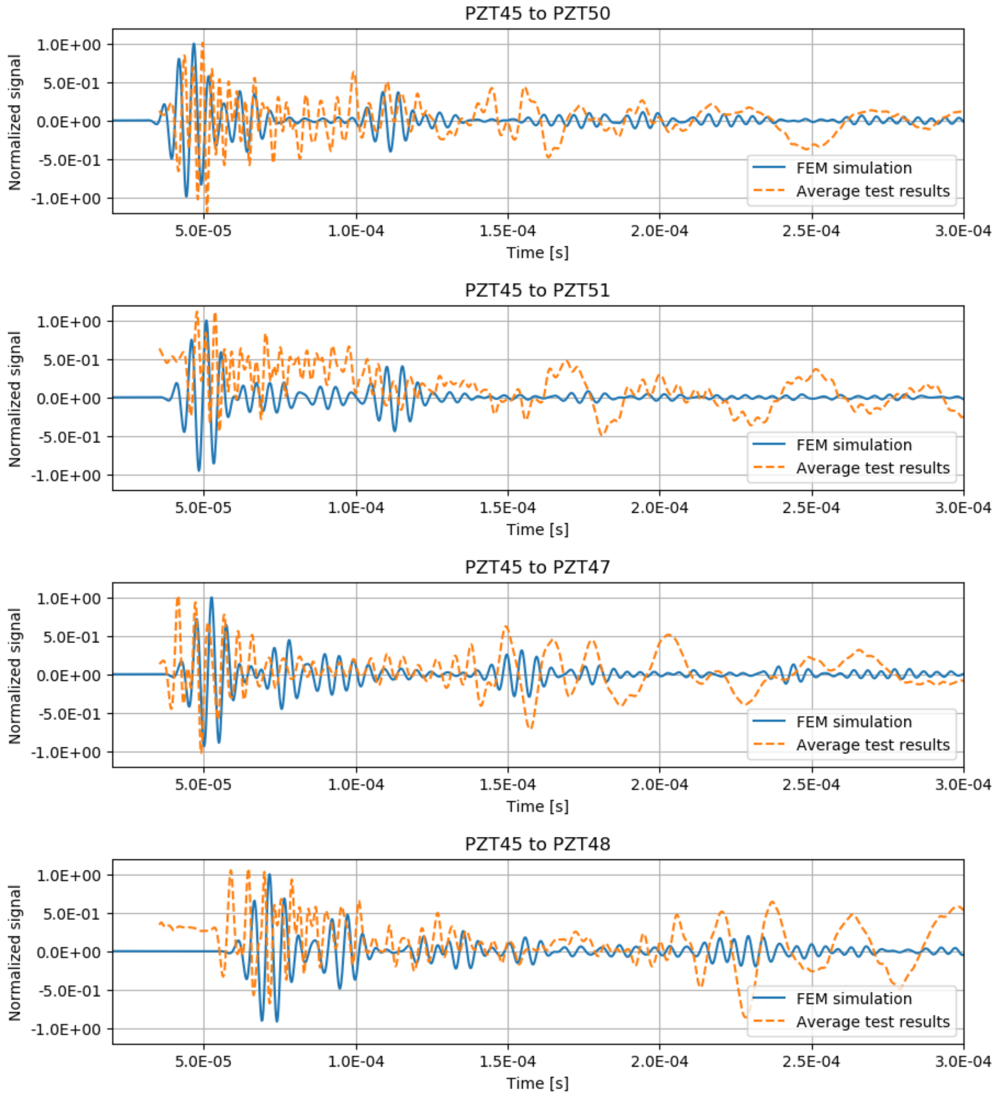

Figure 14: Active interrogation results for the GRA structure - Actuator PZT45 (1/2).

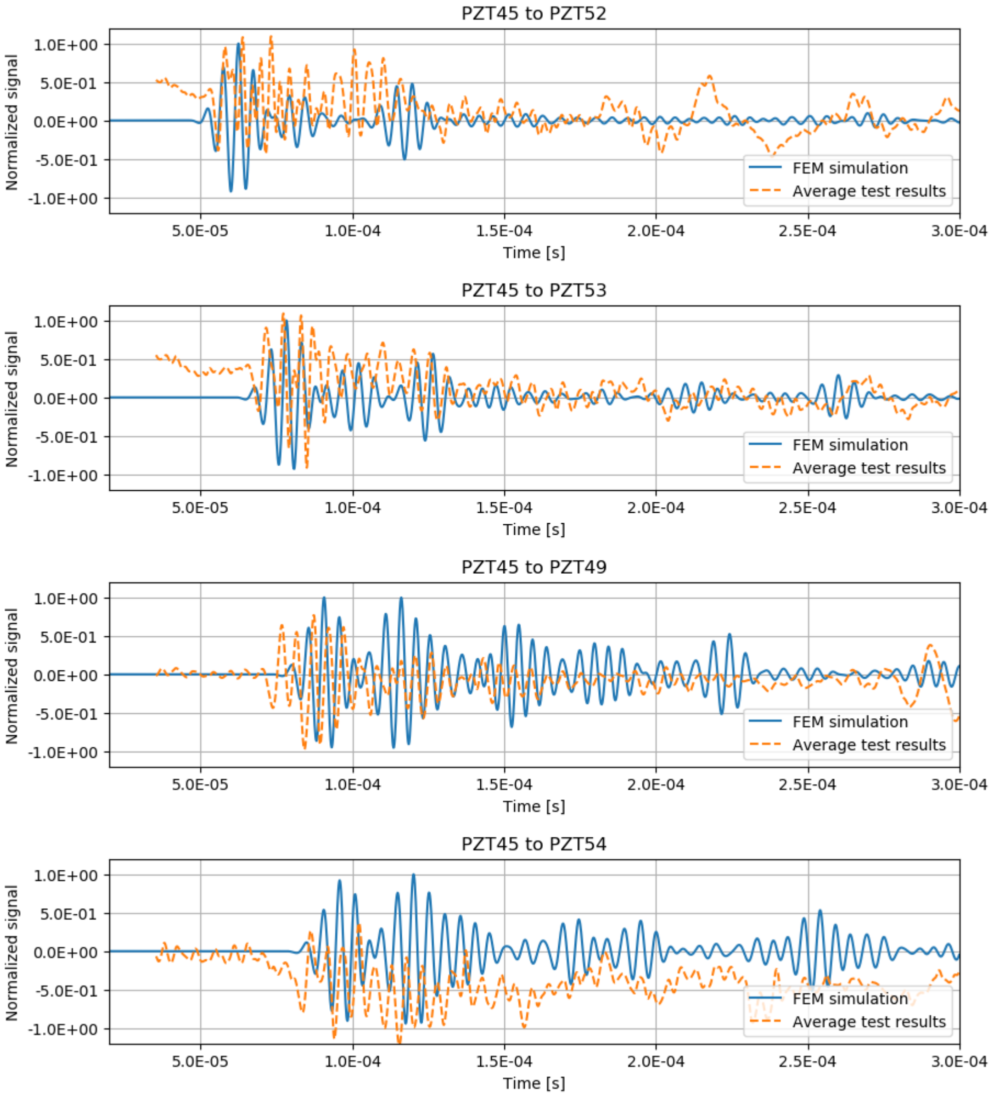

Figure 15: Active interrogation results for the GRA structure - Actuator PZT45 (2/2).

DOI: 10.13009/EUCASS2019-671

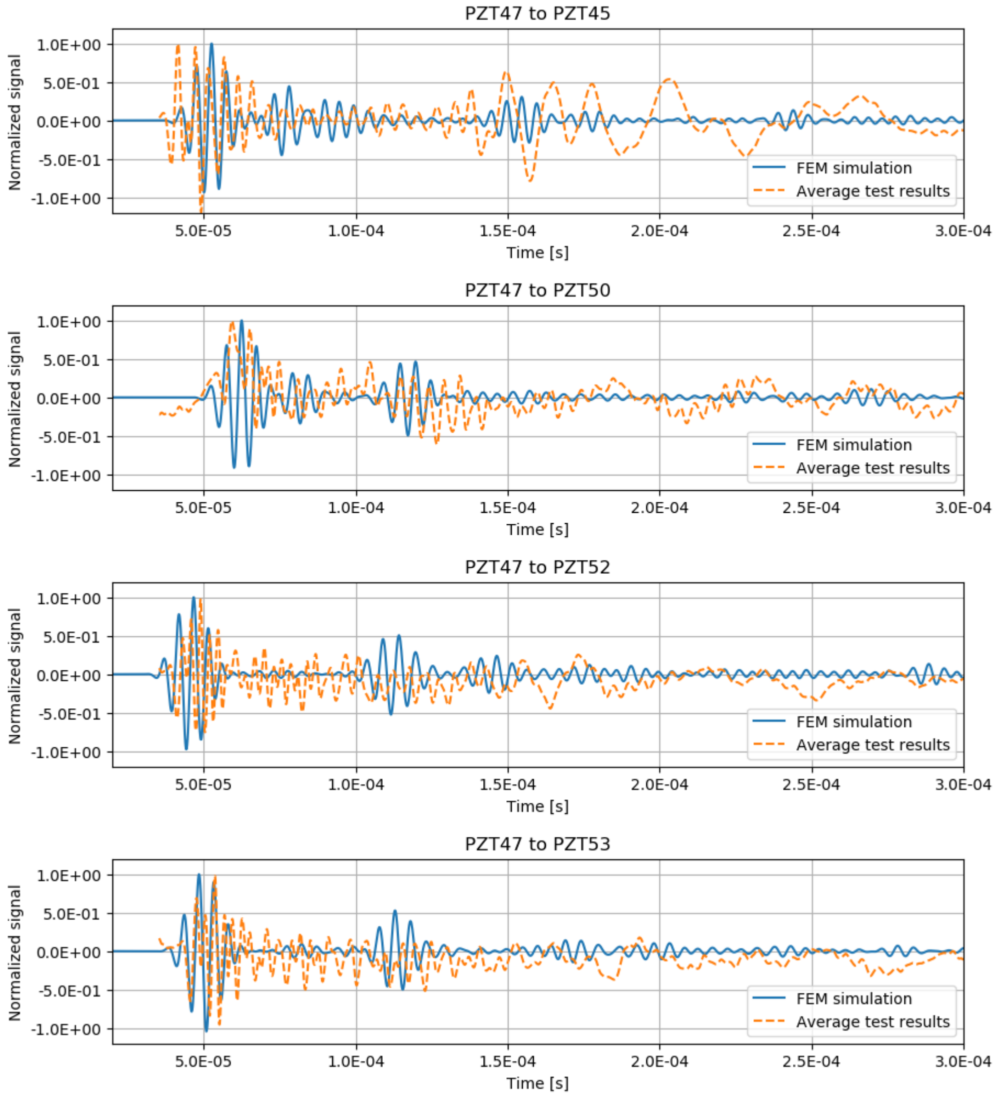

Figure 16: Active interrogation results for the GRA structure - Actuator PZT47.

DOI: 10.13009/EUCASS2019-671

4. Conclusions

This report presents a complex numerical simulation able to represent accurately the Lamb waves on real composite structures and its possible interaction with structural details, and an interpretation of the low energy impact tests results to obtain the damping parameters usable for the FEM model simulation; this damping results may be used to more accurately represent by FEM the passive mode of operation of the system.

The simulations are able to represent accurately the S0 wave and the wave speed is verry accurately captured, however the A0 wave seen in the tests do not achieve the same degree of correlation with the FEM model; additionally, the effect of the stiffener is still not fully represented on the simulation and further work may be necessary to include all significant factors to represent it accurately; main reasons for this discrepancy could be due to the effects of the stiffener adhesive that has not been included in the simulation. Future studies may be performed to quantify the energy dissipated in the stringer interface and develop a methodology to include it in the simulation.

The correlation between the simulation and test results is a difficult task as many parameters introduce uncertainty in the model and in the data acquisition process. A better characterization of the material properties and the stiffener interface with the panel is needed for improve the simulation of future specimens.

Knowledge of the physical problem is key to correlate simulations and tests. Having a database of both can help to develop artificial intelligence models to characterize real in-service events.

5. Acknowledgments

Activities reported in this paper are being developed in the frame of the European Community Seventh & Eight Framework Programs, where Airbus Defence and Space S.A.U. has been partner of Clean Sky 1 Green Regional Aircraft and also remains in Clean Sky 2 as member of Airframe Integrated Technology Demonstrator continuing the research. The Technical University of Madrid (Spain) participates under contract and collaboration with Airbus Defence and Space S.A.U. in support of SHM technology development.

DOI: 10.13009/EUCASS2019-671

References

[1] Joshua P. Ayers, David W. Greve, and Irving J. Oppenheim. Energy scavenging for sensor applications using structural strains. In *Smart Structures and Materials*, volume 5057. SPIE, August 2003.

[2] Alan A. Baker and Murray L. Scott. *Composite Materials for Aircraft Structures, (AIAA Education)*. AIAA American Institute of Aeronautics & Astronautics, 3 edition, September 2016.

[3] Rakesh Chandra, S.P. Singhb, and K. Guptac. A study of damping in fiber–reinforced composites. *Journal of Sound and Vibration*, 262:475–496, May 2003.

[4] J. M. Curtis and D. R. Moore. Fatigue testing of multiangle laminates of cf/peek. *Composites*, 19:446–455, 1988.

[5] Abderrahmane Djabali, Lotfi Toubal, Redouane Zitoune, and Saïd Rechak. An experimental investigation of the mechanical behavior and damage of thick laminated carbon/epoxy composite. *Composite Structures*, 184:178–179, January 2018.

[6] Alper Erturk and Daniel J. Inman. *Piezoelectric Energy Harvesting*. John Wiley & Sons, Ltd., 1 edition, 2011.

[7] R. F. Gibson and S. J. Hwang. Micromechanical modeling of damping in composite including interphase effects. In *36th international SAMPE symposium*, San Diego, CA, April 1991. Covina, CA: Society for the Advancement of Material and Process Engineering (SAMPE).

[8] Matthieu Gresil and Victor Giurgiutiu. Prediction of attenuated guided waves propagation in carbon fiber composites using rayleigh damping model. *Journal of Intelligent Material Systems and Structures*, 26(16):2151–2169, November 2014.

[9] S. Guinard, O. Allix, D. Guedra-Degeorges, and A. Vinet. A 3d damage analysis of low velocity impacts on laminated composites. *Composites Science and Technology*, 62:585–9, March 2002.

[10] F. Sánchez Iglesias, J. García Alonso, R. Tejerina Hernanz, E. Oslé, M. Iglesias Vallejo, L. S. Lorente, J. García Etxebarria, D. Alonso Fernández, A. Lozano, P. Fernández Díaz, B. Larra naga, A. R. Pozo, and A. Fernández López. Numerical simulation and improved correlation techniques for low energy impact detection and damage characterization with elastic waves on composite structures. In *Proceedings of the NAFEMS World Congress 2017*, page 584, June 2017.

[11] Charles H. Keilers Jr. and Fu-Kuo Chang. Identifying delamination in composite beams using built–in piezoelectrics: Part i–experiments and analysis. *Journal of Intelligent Material Systems and Structures*, 6(5):649–663, 1995.

[12] J. M. Kenny and M. Marchetti. Elasto–plastic behavior of thermoplastic composite laminate under cyclic loading. *Composite Structures*, 35:375–382, 1995.

[13] J. Kocbach. *Finite Element Modeling of Ultrasonic Piezoelectric Transducers. Influence of geometry and material parameters on vibration, response functions and radiated field.* PhD thesis, University of Bergen, Dpt. of Physics, 2000.

[14] Horace Lamb. On waves in an elastic plate. In *Proceedings of the Royal Society, A: Mathematical, Physical and Engineering Sciences*, volume 93, pages 114–128, 1917.

[15] Xi Li, Dayou Ma, Huifang Liu, Wei Tan, Xiaojing Gong, Chao Zhang, and Yulong Li. Assessment of failure criteria and damage evolution methods for composite laminates under low–velocity impact. *Composite structures*, 207:727–739, January 2019.

[16] Mark Lin, Xinlin Qing, Amrita Kumar, and Shawn J. Beard. Smart layer and smart suitcase for structural health monitoring applications. In *SPIE Smart Structures and Materials + Nondestructive Evaluation and Health Monitoring*, volume 4332, pages 98–106, June 2001.

[17] Wieslaw Ostachowicz, Pawel Kudela, Pawel Malinowski, and Tomasz Wandowski. Damage localisation in plate–like structures based on pzt sensors. *Mechanical Systems and Signal Processing*, 23:1805–1829, August 2009.

[18] C. Ramadas, Krishnan Balasubramaniam, Avinash Hood, Makarand Joshi, and C.V. Krishnamurthy. Modelling of attenuation of lamb waves using rayleigh damping: Numerical and experimental studies. *Composite Structures*, 93:2020–2025, July 2011.

DOI: 10.13009/EUCASS2019-671

[19] L. Rayleigh. *Theory of Sound (two volumes)*. Dover Publications, New York, 2 edition, 1877.

[20] Hongliang Tuo, Zhixian Lu, Xiaoping Ma, Jun Xing, and Chao Zhang. Damage and failure mechanism of thin composite laminates under low–velocity impact and compression–after–impact loading conditions. *Composites Part B*, 163:642–654, April 2019.

[21] J. Wang, H. Wang, B. Chen, H. Huang, and S. Liu. A failure mechanism based model for numerical modeling the compression–after–impact of foam–core sandwich panels. *Composites Science and Technology*, 151:258–67, October 2017.

[22] Yi Yang, Ching-Tai Ng, Andrei Kotousov, Hoon Sohn, and Hyung Jin Lim. Second harmonic generation at fatigue cracks by low–frequency lamb waves: Experimental and numerical studies. *Mechanical Systems and Signal Processing*, 99:760–773, July 2018.